Severe Thunderstorm Evolution and Mesocyclone Structure as Related to Tornadogenesis

LESLIE R. LEMON AND CHARLES A. DOSWELL III

Techniques Development Unit, NSSFC, Kansas City, MO 64106

(Manuscript received 11 December 1978, in final form 7 June 1979)

ABSTRACT

Severe thunderstorm evolution is synthesized, using published and unpublished studies of radar, instrumented aircraft, visual and surface observations. These observations reveal the existence of a downdraft (originating at 7–10 km AGL) on the relative upwind side of the updraft. Air decelerates at the upwind stagnation point, is forced downward and mixes with air below which then reaches the surface through evaporative cooling and precipitation drag. The initially rotating updraft is then transformed into a new mesocyclone with a divided structure, in which the circulation center lies along the zone separating the rear flank downdraft from the updraft. This process appears to result, in part, from tilting of horizontal vorticity into the vertical. It is proposed that the zone of strong vertical velocity gradient across which the mesocyclone comes to be positioned is also characterized by a strong temperature gradient and is the genesis region of strong tornadoes. Although no direct observations are available yet, we further propose that the strong temperature contrast plays a potential modulating role in tornadogenesis by solenoidal generation of vorticity, in analogy with the extratropical cyclone, to which the transformed mesocyclone bears a striking resemblance.

1. Introduction

The tornado vortex is one of the atmosphere's most intense concentrations of vorticity. For a typical violent tornado with a maximum tangential speed of 100 m s^{-1} at a radius of 100 m, the vertical component of vorticity is 2 s^{-1}. The means by which such vorticity is developed within a thunderstorm are not completely understood. A parcel's vertical component of vorticity can be changed by vortex stretching (implying a vertical gradient of vertical velocity), by tilting of vorticity about a horizontal axis into the vertical (implying a horizontal gradient of vertical velocity), by baroclinic generation via isobaric–isoteric solenoids and by viscous effects.

As documented by Palmén and Newton (1969, p. 237) and clearly developed by Gubin (1962) and others in discussions concerning vorticity, there is an intimate linkage between cyclogenesis and frontogenesis. Gubin's treatment of this subject is on the scale of the extratropical cyclone, placing great emphasis on the role played by vertical motion or, more specifically, by the horizontal gradients of vertical motion. Gubin points out that on the large scale, vertical shear of the horizontal wind (which gives rise to vorticity about a horizontal axis) is largely a result of the thermal wind. Therefore, baroclinic effects are included implicitly in the tilting term, as well as explicitly in the solenoid term of the vorticity equation. Even though the solenoid term disappears from the vorticity equation in pressure coordinates, baroclinic forcing remains via the tilting term. Thus, baroclinic zones which can modify the synoptic-scale vorticity field are associated with significant horizontal gradients of vertical velocity.

This paper addresses phenomena on the scale of the thunderstorm, which is referred to hereafter as mesoscale. However, the resemblance of the severe thunderstorm flow to that of the synoptic-scale disturbance is noteworthy. In fact, Ludlam (1963) has stated "with only alternations in scale, especially the horizontal, . . . (thunderstorms resemble) the dominant form of convection in the presence of shear, (which is) the large-scale baroclinic disturbance". Numerous studies have since revealed a remarkable resemblance of the mesocyclone (Brooks, 1949) to the extratropical cyclone. Examples include Kessler (1970), Lemon (1970, 1976) and Barnes (1978). Analogies with the extratropical cyclone are possible for many mesoscale features, including the vertical motion patterns, the precipitation distribution, and the horizonal flow field. In low levels where the majority of observations have been made, thermodynamic and kinematic similarities have been found through much of the evolution, from genesis through occlusion and decay. Others have also called attention to some aspects of the analogy (e.g., Danielsen, 1975; Burgess *et al.*, 1977; Brandes, 1977a). It is not our intent to infer

dynamic similarity in the strict sense of the term. An extratropical cyclone is quasi-geostrophic and hydrostatic, and vector winds at any level are predominantly two dimensional. Mesoscale flows are ageostrophic and substantially nonhydrostatic, and the vector winds are definitely three dimensional. Nevertheless, the many resemblances are interpreted to suggest there may be a physical concept which links these vortical flows.

This concept of the mesocyclone and a consistent, though somewhat modified, model of the "supercell" tornadic thunderstorm (Browning, 1964) is developed by a synthesis of results and observations from previously published and unpublished studies. The proposed supercell thunderstorm model contains an intense updraft and two downdrafts as the main structural features. One downdraft is located in the precipitation cascade region downwind (relative to the 3–5 km AGL flow) of the updraft. The other downdraft lies immediately upwind of the updraft (relative to the 7–10 km AGL flow). It is the upwind or "rear flank" downdraft which is hypothesized to be of critical importance to mesocyclone structure, storm evolution and tornadogenesis.

More precisely, we propose that air decelerates at the upwind stagnation point of the intense blocking updraft and is forced downward, mixing with air from below which reaches the surface through evaporative cooling of cloud and precipitation droplets and, perhaps, through precipitation drag as well. The initially rotating updraft is disrupted and becomes half of a new mesocyclone with a divided structure, in which the circulation center lies along the zone separating the rear flank downdraft from the updraft. The resulting surface mesocyclone resembles strongly the extratropical cyclone. Although only limited quantitative data exist, the data can be interpreted to show that the zone of strong vertical velocity gradient across which the mesocyclone comes to be positioned is of significant vertical extent, is characterized by strong temperature gradients and is where genesis of intense tornadoes occurs.

Thus, in this modified supercell model, tornadogenesis is associated with a large horizontal gradient of vertical velocity. This suggests that vortex tilting may be an important source of mesocyclone and tornadic vorticity (e.g., Schlesinger, 1978). Further, in analogy with the extratropical cyclone, solenoidal effects may have a significant modulating role.

The information used to develop this concept includes Doppler radar, aircraft, mesoscale surface network, and visual observations. However, a dearth of definite information exists about the three-dimensional wind, temperature and pressure fields in and near tornadic thunderstorms. Even Doppler radar-derived velocity fields are inadequate for this purpose, because of spatial and temporal resolution limitations and because they give no information about the flow outside the precipitation-filled portions of the storm. Further, available thermodynamic data aloft within and near severe thunderstorms are insufficient for direct evaluation of solenoidal effects. Therefore, the proposed supercell storm structure and tornadogenetic mechanism is to be considered as an alternative that fits available observations of stronger tornadoes, rather than a rigorously developed and verified concept.

2. The supercell and mesocyclone life cycles

Beginning with the Thunderstorm Project (Byers and Braham, 1949), a growing body of quantitative knowledge concerning thunderstorms has developed. Because of their impact, severe thunderstorms have received the most attention. However, their relative rarity at any given location and the hazards involved in direct measurements have prevented truly adequate observations. Thus, indirect sensors, primarily radar, have been the basic tools in developing our current understanding. The recent advent of Doppler radar has greatly enhanced our knowledge.

Computer thunderstorm simulations in three spatial dimensions (e.g., Klemp and Wilhelmson, 1978) are progressing but are constrained by both the complexity and magnitude of the problem, and the lack of corroborative observational data. As a consequence of the lack of quantitative information for flows in and near the storms, most thunderstorm models are conceptual (e.g., Newton, 1963; Browning, 1964; Marwitz, 1972a,b).

Attention is focused here on the supercell type of severe thunderstorm, as it is the most prolific producer of tornadoes (Browning and Foote, 1976; Nelson, 1976).[1] Several aspects of the evolving (as opposed to the relatively rare quasi-steady) supercell are pertinent. This type of storm has been investigated extensively by Brown *et al.* (1973), Lemon *et al.* (1975, 1978), Burgess *et al.* (1977) and Donaldson (1978). Information is also drawn from Lemon (1977), who has examined in detail the evolution of nearly 30 supercell storms as portrayed by WSR-57 radar and surface severe weather occurrence data. While the following discussion emphasizes the general evolution, it is recognized that there are always exceptions to the rule. Some of the details of the evolution have been omitted for brevity.

A supercell storm typically begins as a multi-

[1] It is assumed that these storms contain a mesocyclone and, indeed, Browning (1977) suggests this.

cellular, non-severe thunderstorm, moving somewhat slower than, but in the general direction of the mid-level (~700–500 mb) flow. During the first stage of supercell evolution, a cell on the right rear flank develops a mid-level radar echo overhang and weak echo region (WER) (Chisholm, 1973). The echo overhang is a result of the development of a strong persistent updraft and correspondingly strong divergence at the updraft summit. During this stage, the typical storm slows down and turns to the right of the flow at all levels and a supercell is born. The top of the new supercell rises substantially and the WER expands, indicating that the updraft has further intensified.

The second stage of the supercell life cycle is most clearly defined when a bounded WER (BWER) is detected. This is an indication of increasing water and ice content around the updraft core and also, apparently, of continued updraft intensification. At this time, the mesocyclone forms (at 5–8 km AGL), and a tangential velocity profile which resembles that of a Rankine combined vortex (Milne-Thomson, 1968) in single-Doppler data is revealed. The typical mesocyclone has a quasi-solid body core circulation (again, as portrayed in single-Doppler data) 5–10 km in diameter. Initially, the circulation is colocated with the developing BWER and is dominated by updraft. During this stage, and at the onset of the third stage, the largest surface hailfall generally occurs and funnel clouds are often observed (Brown *et al.*, 1973; Lemon, 1977). Occasionally, these funnels reach the surface as relatively weak tornadoes.

The third and final stage of supercell evolution is its collapse phase (Brown *et al.*, 1973; Lemon, 1977; Lemon *et al.*, 1977, 1978). It is most easily recognized by increasing radar reflectivity in the BWER. Dissipation of the BWER, decreasing overhang and lowering of the storm's radar as well as visual cloud top occurs. The storm's downdrafts increase in both magnitude and extent while the updraft is decreasing. The referenced literature (see also Brandes, 1978) indicates that *it is not until this time that the strongest tornadoes and straight-line winds (or "downbursts") occur.*

Details of supercell evolution have been clarified by Doppler radar observations. While vertical velocities obtained by vertical integration of the horizontal Doppler velocity divergence are somewhat uncertain, especially above mid-levels (Ray and Wagner, 1976), the basic patterns appear to be reliable. For example, the vertical draft configuration depicted by dual-Doppler-derived vertical velocity fields is in agreement with aircraft measurements (Marwitz, 1972a,b) and numerical simulations (Schlesinger, 1978). In particular, downdrafts have been noted on both the upwind and downwind[2] flanks of the supercell's updraft.

Doppler data also reveal a separation of the mesocyclone core circulation from the BWER (and principal updraft), prior to or during BWER collapse (Burgess *et al.*, 1977; Lemon *et al.*, 1978). This separation results in an upwind displacement of the mesocyclone relative to the BWER, such that the circulation center lies within the storm's precipitation-filled volume (Lemon *et al.*, 1978). Further, after separation the mesocyclone is positioned across the zone of strong vertical velocity gradient between the updraft and the rear flank downdraft (e.g., Burgess *et al.*, 1977; Brandes, 1978). Near the time of separation, the mesocyclone descends to the surface. Descent of the circulation occurs simultaneously (within the limits of temporal resolution) with the descent of the rear flank downdraft.

Shifting the mesocyclone center from near the updraft center to the zone of high vertical velocity gradient implies a basic change in the nature of the mesocyclone. The early mesocyclone is apparently

[2] References to upwind and downwind refer to the storm-relative 4–10 km flow.

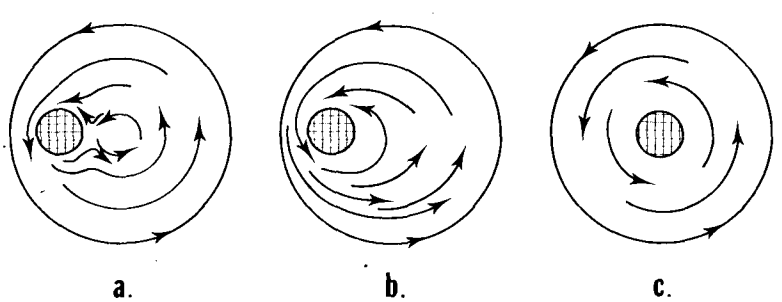

FIG. 1. Proposed relationship of the developing tornadic vortex signature, TVS (stippled), to the mesocyclone core circulation in the Union City, Oklahoma storm at 5 km AGL on 24 May 1973 (after Lemon *et al.*, 1978). In (a), dry relative environmental winds approach the mesocyclone from 271° at 6 m s^{-1} (i.e., from the left in the figure). Shown in (b) is the replacement of a weakening circulation near the core center by flow around the strengthening TVS. Mesocyclone transformation is complete in (c), in which the TVS is located at the core center.

a rotating updraft, whereas the transformed mesocyclone has a divided structure, with strong cyclonically curved updrafts to the east in the "warm inflow sector" and strong cyclonically curved downdrafts to the west in the "cool outflow sector". This is a significant modification of the existing mesocyclone concepts (e.g., Burgess and Brown, 1973; Fujita, 1973; Davies-Jones and Kessler, 1974) which have interpreted the mesocyclone only as a rotating updraft. This divided mesocyclone structure is distinct from the "twisting downdraft" proposed by Fujita (1973), in which the downdraft is upwind and adjacent to the mesocyclone (still seen as a rotating updraft).

Most significant tornadoes in the referenced literature develop at the mesocyclone center and touch down near the tip of the "occlusion," close to the updraft-downdraft interface, as seen in Burgess *et al.* (1976, 1977), and Brandes (1977b, 1978). The referenced papers also note secondary tornadoes or mesocyclones, observed along the trailing gust front associated with the rear flank downdraft. Thus, in the few well-documented storms to date, *most tornadoes have reached the surface only after the mesocyclone has developed a divided structure.*

When the thunderstorm mesocyclone is considered as it progresses from genesis through occlusion, the analogy with the extratropical cyclone becomes apparent. In fact, when the storm flow structure is viewed in a storm-relative sense (as considered in Section 5) the analogy is striking [e.g., Palmén and Newton (1969), their Fig. 10.20 and accompanying discussion]. Even the secondary mesocyclone or tornado occurrences along the trailing gust front can be considered small-scale analogies to waves along a synoptic-scale cold front.

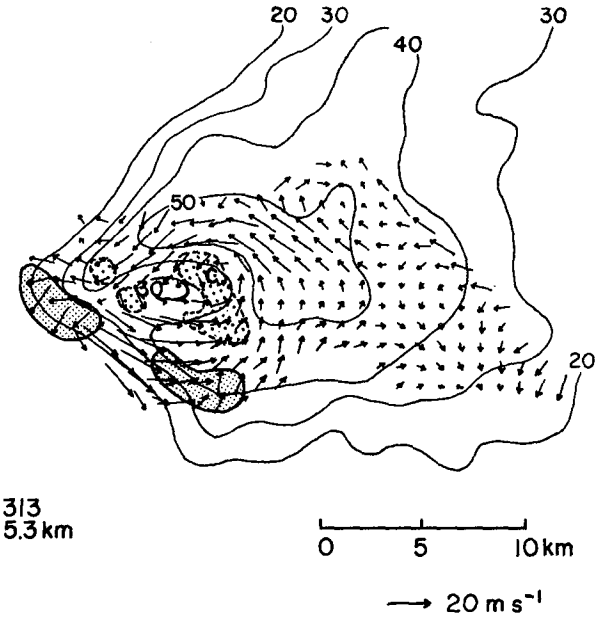

Fig. 2. Perturbation winds and reflectivities (solid lines) for Oklahoma City storm, 8 June 1974, after Burgess *et al.* (1977). Reflectivity contours are in 10 dBZ intervals beginning at 20 dBZ. Wind vector length equal to grid spacing is 10 m s^{-1}. Fine stippling indicates downdraft and coarse stippling updraft as calculated by integration of continuity equation. Circulation centers are marked by (c). Time (CST) and altitude are indicated at lower left.

3. Characteristics of tornadogenesis in supercell thunderstorms

It has been necessary to clarify the structure of the mesocyclone because it is critically important in the generation of strong tornadoes. Here we discuss in more detail the data and observations that have led us to our present view of the relationship of tornado development to the structure and evolution of the storm as a whole.

a. Radar characteristics

Doppler radar examinations of tornadic storms frequently reveal a small region of strong horizontal shear, the tornadic vortex signature (TVS), preceding by tens of minutes the tornado touchdown (Brown *et al.*, 1978). During the Union City, Oklahoma storm of 24 May 1973, the TVS first developed in mid-levels on the upwind periphery of the BWER and its coincident mesocyclone 23 min prior to tornado touchdown. In subsequent data, the circulation was found in a region of relatively high radar reflectivity, upwind of the collapsing BWER. The TVS was then located at the mesocyclone center. It has been suggested (Lemon *et al.*, 1978) that in this case, the TVS may be a separate small, but intense, circulation center that strengthens rapidly, expanding until it dominates and eventually replaces the original mesocyclone core. This development is illustrated schematically in Fig. 1. However, the TVS and mesocyclone center may also maintain separate identities (Ray *et al.*, 1976; Brandes, 1978).

Multiple-Doppler measurements also indicate that the descent of both the mesocyclone and TVS is closely related to the development of the rear flank downdraft. During the 8 June 1974, Oklahoma City tornado, Burgess *et al.* (1977) have found that at 1313 CST the mesocyclone core was initially centered in updraft at mid-levels (Fig. 2). At this time, the rear flank downdraft was just developing at that level (concurrent surface data give no indications that it had yet reached the surface). During the next dual-Doppler observation at 1357 (single-Doppler data, collected at 1335, provide evidence for the inferred structural continuity), after the storm had produced the first of three tornadoes, the mesocyclone core was located

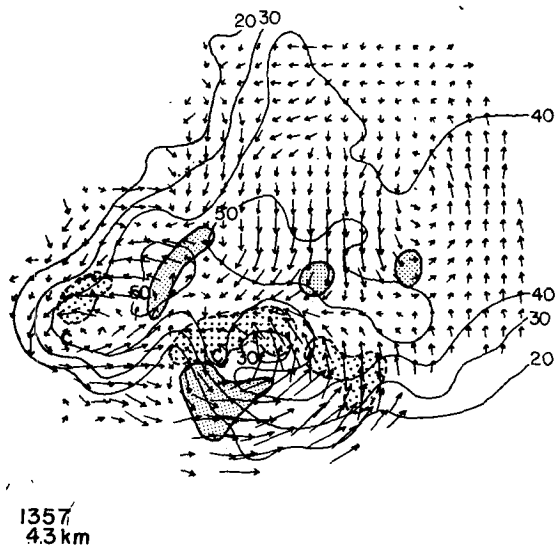

FIG. 3. As in Fig. 2.

about 5 km upwind of the slowly collapsing BWER, lying in the zone of strong vertical velocity gradient (Fig. 3). The TVS was found at the mesocyclone center and, therefore, also within the strong vertical velocity gradient. This draft-mesocyclone relationship had vertical continuity from the surface to at least 6 km AGL and was maintained throughout tornado production. With the exception of a weak tornado on the gust front south of the mesocyclone, each tornado had an associated TVS and was located in the vertical velocity gradient after the mesocyclone had developed a divided structure and reached the surface. Brandes (1978) has presented additional Doppler analyses (for this and another storm) compatible with these observations. Specifically, he found the tornadoes were each within the vertical velocity gradient between updraft and downdraft. Note that the data suggest that while the tornado occurs within the strong vertical velocity gradient, it is probably located on the updraft side of that gradient.

Further support for the contention that strong mesocyclone-associated tornadoes are located on the vertical velocity gradient comes from the relationship of the radar-detected hook echo to this transition zone. The hook echo has long been recognized to be directly associated with tornado location (e.g., Huff *et al.*, 1954; Garrett and Rockney, 1962; Brown *et al.*, 1973). Those few Doppler radar observations, surface analysis, and aircraft penetrations of hook echoes obtained thus far (Burgess *et al.*, 1977; Marwitz, 1972a, b) consistently show that the hook echo is located in a region of high vertical velocity gradient, strong temperature gradient (at least in low levels where those data are available), and somewhat behind the surface windshift line associated with the rear flank downdraft.[3] In fact, as early as 1969 (Haglund, 1969), it was concluded that the hook echo trails the surface wind

[3] Marwitz (1972a, b) has found the strongest updrafts a few kilometers ahead of the hook echo, near the surface wind shift line.

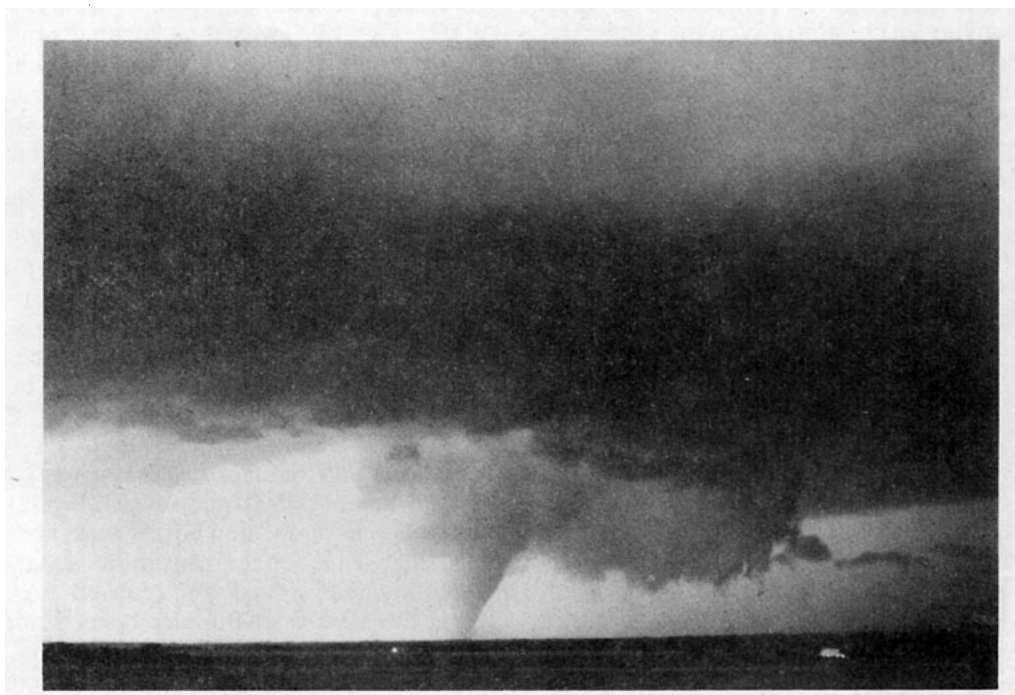

FIG. 4. The 24 May 1973 Union City tornado at maturity viewed from east, showing tornado near the south (and west) edge of wall cloud and closely associated clear slot to the left and rear in photograph (from Moller *et al.*, 1974).

FIG. 5. Last of the Oklahoma City storm tornadoes 8 June 1974, viewed from the southeast. The downdraft-associated "clear" slot or region of higher sunlight cloud base is shown to the left and updraft-associated, lowered cloud base is visible to the right of the tornado (from Burgess *et al.*, 1977).

shift slightly, and is associated with the boundary between updraft and downdraft.

b. Visual characteristics

A lowered rain-free cloud base frequently associated with severe thunderstorms and tornadoes (referred to as a wall cloud by Fujita, 1960) has been shown by Marwitz *et al.* (1972) and others to indicate updraft. Field observations reveal that tornadoes are usually not centered within but, rather, located beneath the right or rear periphery of the wall cloud (e.g., Figs. 4, 5 and 6). Photographs of tornadoes also often reveal a nearby region of less dense cloud or relatively clear air, originally seen immediately to the rear or right rear of the tornado, which eventually spreads or propagates around the funnel, as described in detail by Moller *et al.* (1974). This region, which we call a "clear slot", is evident in Figs. 4 and 5, and additional examples may be found in Stanford (1977), Peterson (1976) and Beebe (1959). The clear slot shown in Burgess *et al.* (1977) is also found to be associated with a radar-indicated downdraft and a hook echo. Perhaps large, precipitation-sized droplets are present in the downdraft, and are brought down from the echo overhang, even though the air contains only ragged clouds or is visibly cloudless in low levels. If so, since radar reflectivity is more strongly dependent on the size than on the number of droplets, radar may show substantial echo in the "clear" slot. As suggested by Moller *et al.* (1974) and Burgess *et al.* (1977), *the clear slot is the visual manifestation of the rear flank downdraft.*

During the development and evolution of tornadoes, clouds around the rear and right periphery of the funnel may appear to descend and dissipate rapidly (Golden and Purcell, 1977). The region where cloud dissipation has occurred is shown clearly in Fig. 6, for two different tornadoes in their shrinking stage. In the background of both photographs, the dark, uniform cloud base associated with updraft can be seen. During this stage in the Union City case (Fig. 6a), Golden and Purcell (1978) have found photogrammetric evidence that the tornado was positioned between a descending current on the right (or south) quadrant and an ascending current on the left (or north) quadrant. Although they attributed this, at least in part, to vortex tilt, the clear slot to the right of the funnel aloft, within the descending current, suggests that tilt alone does not explain the downdraft. These findings can also be related to the observations of Van Tassel (1955) and Beebe (1959), who have reported cold downdrafts to the immediate right or on the rear of the tornado.

4. Downdraft structure and origin

In Sections 2 and 3, radar, aircraft and visual observations have been discussed which indicate the existence and apparent importance of downdrafts to storm structure and tornadogenesis. Fur-

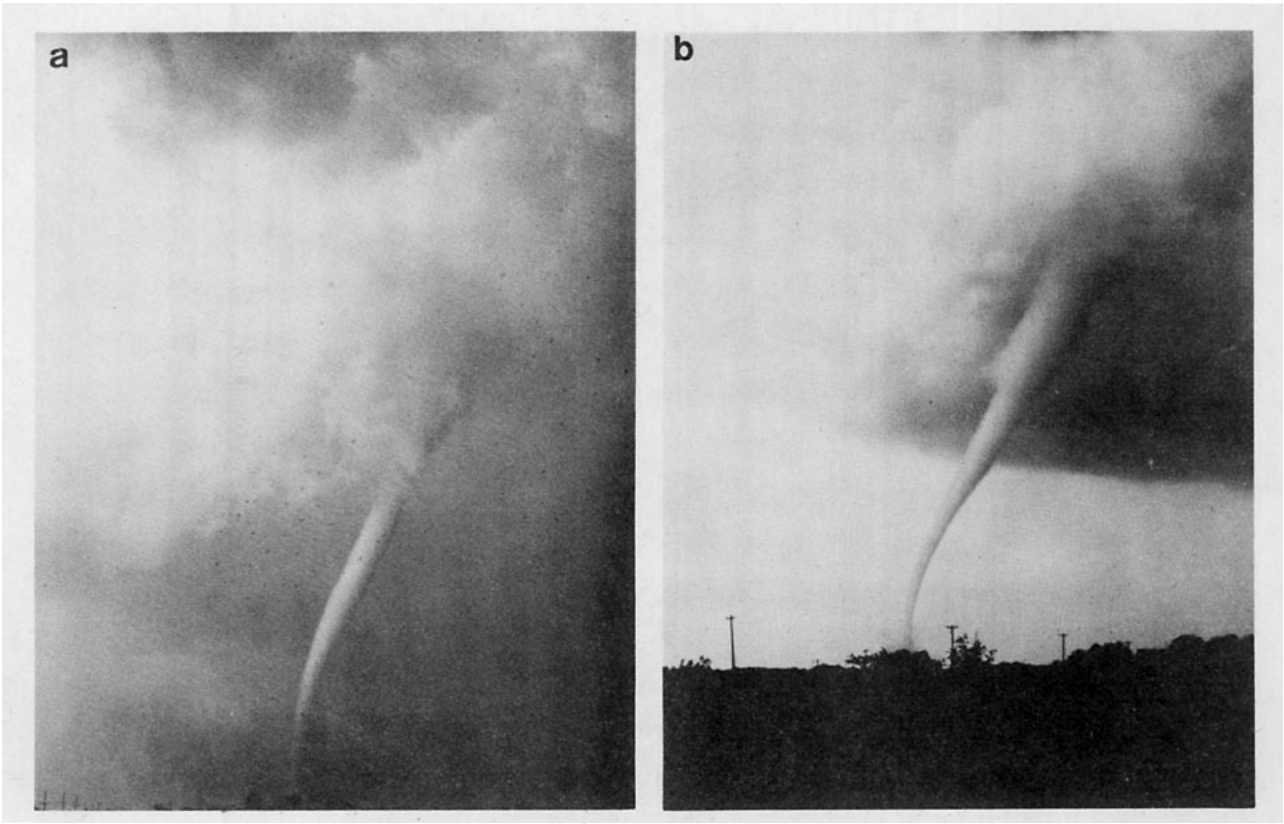

FIG. 6. Strikingly similar appearing tornadoes at (a) Union City, Oklahoma (National Severe Storms Laboratory photo) and at (b) Manhattan, Kansas (from Flora, 1954).

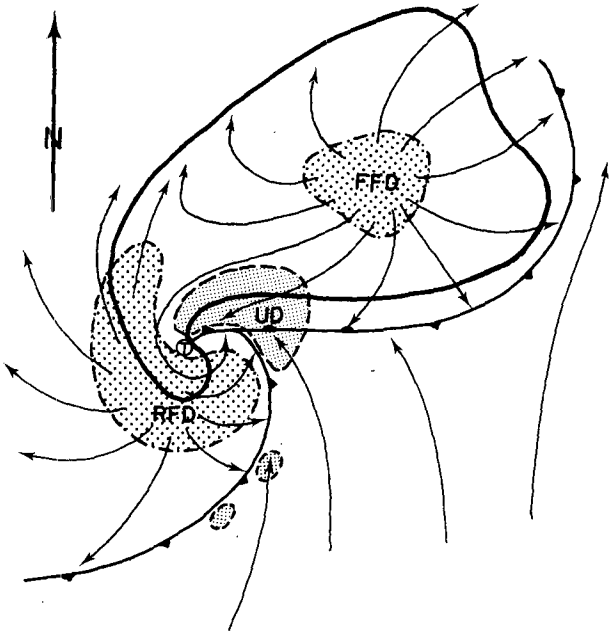

FIG. 7. Schematic plan view of a tornadic thunderstorm at the surface. Thick line encompasses radar echo. The thunderstorm "gust front" structure and "occluded" wave are also depicted using a solid line and frontal symbols. Surface positions of the updraft (UD) are finely stippled, forward flank downdraft (FFD) and rear flank downdraft (RFD) are coarsely stippled, along with associated streamlines (relative to the ground) are also shown. Tornado location is shown by an encircled T.

ther, mesonetwork observations also provide evidence of the two distinct downdrafts associated with supercell storms. Surface air beneath the downwind downdraft has a potential wet-bulb temperature (θ_w) that probably results from mixing of updraft (high θ_w) and mid-level environmental (low θ_w) air (Lemon, 1974). This forward flank downdraft forms a relatively weak discontinuity at the surface on the forward and right flanks of the radar echo. As the storm moves, the discontinuity spreads ahead of the echo, but may become quasi-stationary along the right echo flank (Fig. 7).

The existence and strength of the rear flank downdraft is also revealed by the mesonetwork measurements of Charba and Sasaki (1971), Lemon (1976) and Barnes (1978). These observations show θ_w values compatible with mid-level (3–5 km AGL) environmental air, divergence and strong pressure excesses on the storm's rear flank, immediately trailing hook echoes. This air can generally be dis-

tinguished from forward flank downdraft air because it is drier, more dense, and usually cooler (Lemon, 1974; Nelson, 1977).[4] As the outflow from the rear flank downdraft spreads, its surface discontinuity can interact with the weaker one formed by the rainy downdraft, giving rise to the wave structure (e.g., Barnes, 1978) and apparent "occlusion" found by Lemon (1976). These low-level features are depicted schematically in Fig. 7.

The importance of the rear flank downdraft has previously been emphasized by Nelson (1977). He has studied an originally multicellular, marginally severe hailstorm which was transformed into a much more severe supercell storm (with mesocyclone and hook echo) at the time that it developed a rear flank downdraft. He concludes that in this case the rear flank downdraft originated from 7 km AGL, where the relative environmental wind considerably exceeded that at other levels. Barnes (1978, his Fig. 4) has presented radar data, in addition to the mesonetwork data mentioned above, for a supercell which show a large elliptical echo-free region immediately upwind of the high reflectivity core at 7.5 km AGL. By overlaying the data from 7.5 and 1.5 km (Fig. 8), this echo-free region is seen to be above an echo-weak notch to the immediate rear of the hook echo and low-level reflectivity core. This feature we interpret to reveal the rear flank downdraft, which is evaporating the precipitation and giving rise to an echo-weak (or echo-free) region. Since the region is large and completely echo-free at 7.5 km and the relative environmental winds impinging on the storm's rear flank are increasing with height, we infer that the origin of the rear flank downdraft is at still higher levels, in this case.

Another clue to the rear flank downdraft's origin can be found in the fact that supercell storms are known to travel across mid and upper tropospheric flow (see e.g., Browning, 1964; Charba and Sasaki, 1971). Since they also move slower than this flow, they typically intercept large amounts of the low θ_w air on the right and rear storm flanks. In fact, it has been generally found that the stronger the upper and mid-level relative inflow, the stronger the tornadoes associated with such storms (Darkow and McCann, 1979). As proposed by Newton and Newton (1959), and shown by Doppler measurements (see Lemon *et al.*, 1977), the storm updraft acts as an obstacle to the 4–10 km flow. Thus, the updraft core is essentially undiluted (Heymsfield

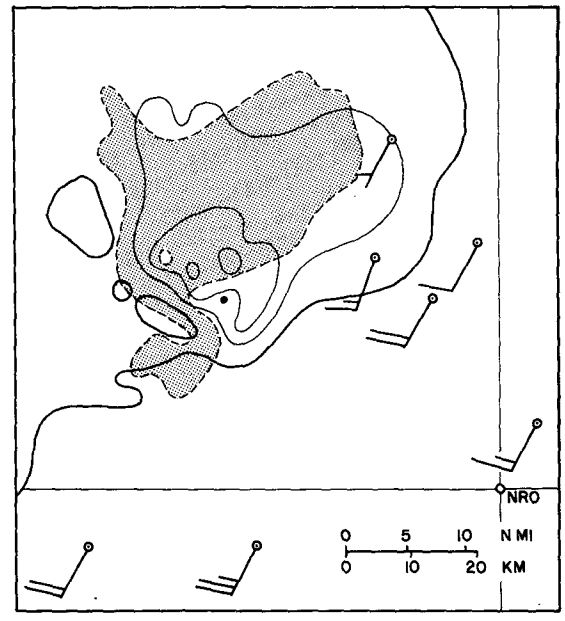

FIG. 8. Superposition of 1.5 and 7.5 km radar reflectivity data from a tornadic supercell thunderstorm (after Barnes, 1978, Fig. 4). Coarse stippling encompasses 32 dBZ or greater reflectivity at 1.5 km, while fine stippling encloses 1.5 km dBZ reflectivity core. The heavy contour shows 15 dBZ reflectivity at 7.5 km, while the fine contours represent 32, 45 and 52 dBZ at that level. The small black dot locates the storm top. Wind data derived from mesonetwork rawinsondes show storm-relative flow at 6.75 km, where one full barb represents 10 m s^{-1}. NRO locates the radar at Norman, Oklahoma.

et al., 1978), with significant entrainment occurring only on its periphery.

It has already been suggested (e.g., Ludlam, 1963; Barnes, 1978) that mid-level relative inflow is the probable source of the rear flank downdraft. As early as 1949 (Sawyer, 1949), it was hypothesized that a downdraft could be initiated by precipitation falling from the rear (upwind) anvil. More recently, Bonesteele and Lin (1978) have suggested that precipitation from the updraft is deposited on the upstream storm flank by the tilt and rotation of the updraft around the mesocyclone, giving rise to the rear flank downdraft shown clearly in their diagnostic model.

It is proposed here that the rear flank downdraft forms when upper mid-tropospheric air (7–10 km AGL) passes beneath the upwind anvil and then impinges on the updraft (Alberty, 1969). The upper mid-tropospheric source is emphasized since Darkow and McCann (1979) have shown that the relative flow at these levels is much stronger than the storm-relative minimum they found at 4 km and because of the evidence obtained from Nelson (1977) and Barnes (1978). Thus, this downdraft may be dynamically forced by the non-hydrostatic

[4] As suggested by Williams (1963), it has been observed that this downdraft can arrive at the surface warmer than its surroundings. When such an event occurs, it may be south of the hook echo (Burgess *et al.*, 1977) or wherever forced descent is less likely to encounter sufficient liquid water to maintain negative buoyancy.

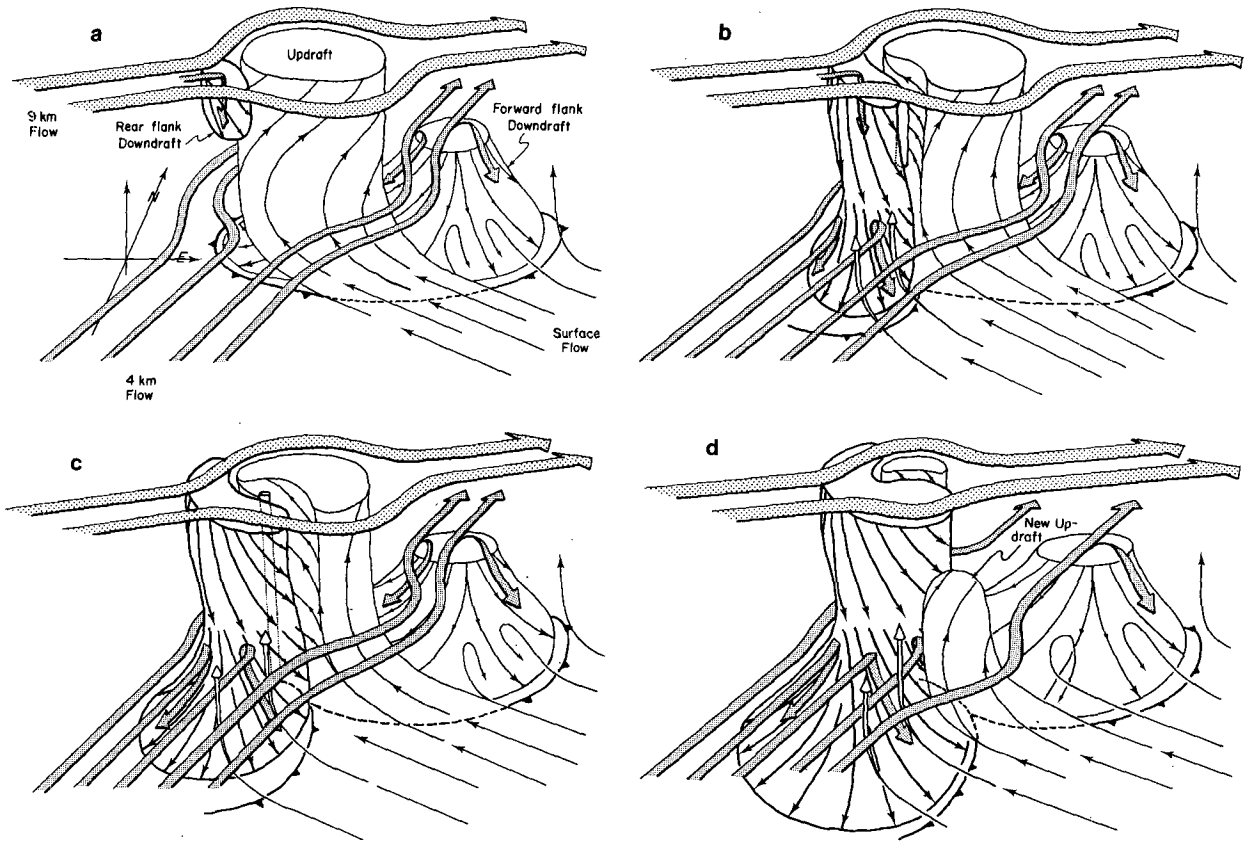

FIG. 9. Schematic three-dimensional depiction of evolution of the drafts, tornado and mesocyclone in an evolving supercell storm. The stippled flow line suggesting descent of air from the 9 km stagnation point has been omitted from (c) and (d), for simplicity. Fine stippling denotes the TVS. Flow lines throughout the figure are storm relative and conceptual only, not intended to represent flux, streamlines, or trajectories. Conventional frontal symbols are used to denote outflow boundaries at the surface, as in Fig. 7. Salient features are labeled on the figure.

component of the vertical pressure gradient, like those formed on the upwind side of tall buildings in strong winds (Melbourne and Joubert, 1971; Wise, 1971).

Further support for this concept may be found in the measurements of Ramond (1978), who has observed significant perturbation pressure excesses near the upwind convective cloud boundary at the stagnation point. Klemp and Wilhelmson (1978) have recently simulated this process in their three-dimensional numerical model.

This approaching ambient flow beneath the upwind cumulonimbus anvil encounters precipitation within and beneath the sloping echo overhang detected on radar and then large concentrations of cloud particles near the updraft periphery. The sloping echo overhang results from the strong divergence at the updraft summit. This divergence forces precipitation into the upwind anvil (as well as the downwind anvil), from which it falls into the ambient flow. Thus, in the severe storm, descent of the air on the upwind flank is initially dynamically forced and then enhanced and maintained through precipitation drag (Clark and List, 1971) and evaporative cooling (Kamburova and Ludlam, 1966). It is not suggested that air from 7 to 10 km AGL actually reaches the surface but rather that the downdraft begins there and mixes with large quantities of air as it descends through middle levels. The result is similar to the "mesoscale unsaturated downdraft" described by Zipser (1977) but on a smaller scale.[5]

5. Observational summary

To summarize the observations, a schematic three-dimensional, storm-relative portrayal of the evolution of the supercell drafts, mesocyclone and tornado is proposed and shown in Figs. 9a–9d. For figure clarity, the vertical scale has been exaggerated and slope of the features is omitted. Also, features above 9 km AGL and the storm radar echo have

[5] Zipser's discussion emphasizes the microphysical details of the downdraft, also suggesting that cloud and small precipitation droplet evaporation is the major factor in causing descent. Schlesinger (1978) has arrived at a similar conclusion via numerical simulation.

been omitted, but are included in the discussion. (The relationship of the drafts to the low-level echo are shown in Fig. 7.) The schematic begins in stage 2 of the storm's evolution, i.e., a strong rotating updraft is present (Fig. 9a), coincident with the BWER. The forward flank downdraft in the precipitation cascade region is already well developed, with some low-level air mixing with this downdraft. At the surface, a gust front on the forward and right echo flanks results. On the relative upwind side of the strong blocking updraft at ~9 km AGL, ambient air encounters cloud and precipitation and is deflected downward at the resulting stagnation point.

A new vortex (divided mesocyclone) is initiated on the enhanced density and vertical velocity gradient between the updraft and the descending rear flank downdraft (Fig. 9b). Why this vortex forms is as yet unclear. As it forms, it is possible that the updraft is disrupted by the new vortex developing on its periphery, thereby decreasing draft strength and leading to BWER collapse. The low-level radar echo develops a pendant or hook echo on its rear flank at this time. An interpretation of pendant development is that descending precipitation particles fall at a rate significantly greater than their individual terminal fall velocities, owing to downward forcing in the rear flank downdraft. Thus, these precipitation particles reach the surface sooner (and further south) than the precipitation in the surrounding portions of the echo overhang. Even though this downdraft is shown as continuous from 9 km AGL to the surface, the air originating there rarely, if ever reaches the surface.

While not clearly apparent in Fig. 9b, the mesocyclone at this time is not a closed vortex, especially when viewed in a storm-relative sense. Instead, on the left updraft flank the cyclonically curving updraft flow is sheared or turned back downwind anticyclonically by the opposing ambient winds and is probably influenced by anticyclonic vorticity produced via tilting in the same region. Fig. 10 displays that storm-relative flow in plan view at upper mid-levels for a period between Fig. 9b and 9c. In most multiple-Doppler analysis (e.g., Burgess *et al.*, 1977), the data presented have been obtained by subtracting the average wind vector over the domain at each height. The result is a *perturbation* wind field at each level, intended to emphasize the vorticity features of the flow. The storm-relative flow is obtained by subtracting the storm motion vector from the field at all levels. When this is done, a flow picture as in Fig. 10 results, which may give a better visualization of the flow within the moving storm and is compatible with the storm-relative Doppler analyses of Brandes (1978). That the majority of updraft trajectories curve anticyclonically has also been proposed by Marwitz (1972a; see his Fig. 19)

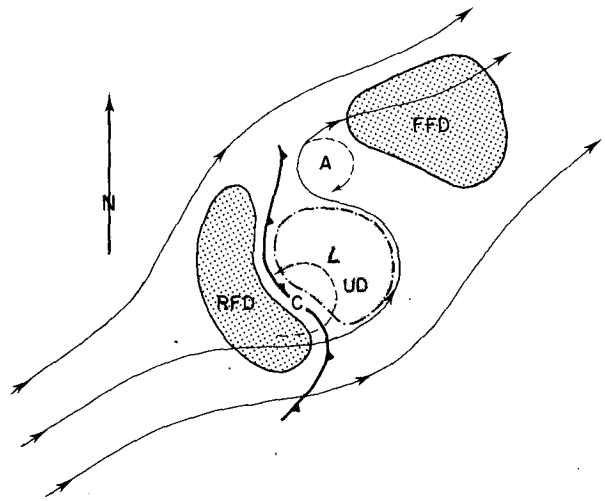

FIG. 10. Storm-relative flow at mid-levels (~7 km) after stage 2 of supercell evolution. The thick barbed line is a strong temperature and vertical velocity interface; updraft (UD) is finely stippled and downdraft, both the forward flank (FFD) and rear flank (RFD), is coarsely stippled. The L is the core of the original mesocyclone and C is the center of the transformed or divided mesocyclone. The A indicates a region of anticyclonic vorticity.

and (after initial cyclonic curvature) by Browning and Foote (1976; see their Figs. 10 and 17). If a closed cyclonic circulation occurs in a storm-relative sense during a storm's lifetime, it is most probable during mesocyclone peak intensity (Brandes, 1978).

As the collapse phase proceeds, the rear flank downdraft reaches the surface, forming a second outflow boundary and giving rise to the wavelike structure of the thunderstorm gust front (Fig. 9b). This second, southward extending boundary forces updrafts along it, as shown, aiding the development of the flanking line of cumulus congestus frequently observed southwest of the supercell storm. Some of the downdraft air is involved in the reorganizing mesocyclone on its right and rear flanks, while the inflow rises cyclonically to the front and left of the new circulation center analogous to the extratropical cyclone. The incipient tornado (TVS) is shown in mid-levels within the developing divided mesocyclone, on the updraft side of the updraft/downdraft gradient.

Low-level occlusion takes place as shown in Fig. 9c (see also the corresponding plan view of Fig. 7). In association with updraft disruption by the now-divided mesocyclone, the collapse of the BWER is nearly complete and the storm top is lowering. The tornado reaches the surface along the leading edge of the density gradient, typically near the tip of the occlusion, as shown here. Low-level "wrap-up" of the radar hook echo takes place and descending precipitation subsequently engulfs the mesocyclone.

Beyond this stage, the updraft weakens as the occlusion continues and the downdraft spreads throughout the mesocyclone, cutting off the inflow (Fig. 9d). The tornado dissipates and, if the storm is to persist, new updraft must develop elsewhere, such as that shown in Fig. 9d southeast of the original updraft. In association with this updraft, the same evolution can take place once again, producing a periodic occurrence of tornadoes (e.g., Darkow and Roos, 1970) from the same storm system.

Although the model presented here has ignored tilt in the draft structures, except perhaps at very low levels, it is recognized that the drafts generally slope in the vertical. However, the available observations and simulations (e.g., Schlesinger, 1978) suggest that tilt of the drafts is not essential to the development of the model structures.

6. Proposed mechanisms of tornadogenesis

a. Existing theories

If this model as presented is substantially correct, then current theories of tornado formation must be reconsidered. To suggest that tornadoes develop through convergence of existing vorticity is questionable when major tornado touchdown occurs with the evolving supercell during *updraft weakening,* and when mesocyclone flow is increasingly dominated by *downdraft.* For instance, the Union City, Oklahoma tornado touched down nearly 30 min after peak storm height and BWER prominence (Lemon *et al.,* 1978). The major Fort Cobb, Oklahoma tornado touched down over 20 min after the most prominent stage of BWER development (indeed, the BWER had filled with high reflectivity echo and was no longer evident) and during descent of the storm top (Lemon, 1977).

Convergent enhancement of vorticity leading to tornadogenesis is also not easily reconciled with models and observations showing the updraft axis between a cyclonic-anticyclonic vortex doublet (e.g., Klemp and Wilhelmson, 1978; Ray *et al.,* 1976). Mesocyclone tornadoes usually occur along the cyclonic vortex axis (e.g., Lemon *et al.,* 1977).

The low-level gust front has also been suggested as the site for tornadogenesis, owing to enhanced convergence and/or the roll-up of kinematic shear instabilities along the quasi-vertical vorticity sheet (Barcilon and Drazin, 1971; Brandes, 1977b). The formation of the TVS (i.e., incipient tornado) at mid-levels appears to rule out such a low-level causal mechanism in the stronger mesocyclone tornadoes.

b. Potential sources for tornadic vorticity generation

Following Petterssen and Austin (1942), consider a coordinate system with the x-axis perpendicular to a baroclinic zone (front), positive toward the cold air. Also, assume that variations along this front are small compared to cross-frontal changes. Thus, an appropriate (inviscid) vorticity equation is

$$\frac{\mathrm{d}}{\mathrm{dt}}\left(\frac{\Delta v}{\Delta x}\right) = -v\frac{\partial f}{\partial y} - fD - \frac{\Delta v}{\Delta x}D$$

(Coriolis) (stretching)

$$-\frac{\Delta w}{\Delta x}\frac{\partial v}{\partial z} - \frac{\Delta \alpha}{\Delta x}\frac{\partial p}{\partial y}, \quad (1)$$

(tilting) (solenoidal)

where v is the horizontal wind component parallel to the front, w is the vertical wind component, f is the Coriolis parameter, D is divergence, α is specific volume and p is pressure.

This equation governs the time rate of change of shear across the front as a result of the various forcing terms. Note that the equation of state requires

$$\frac{\Delta \alpha}{\Delta x} = -\frac{RT_v}{p^2}\frac{\Delta p}{\Delta x} + \frac{R}{P}\frac{\Delta T_v}{\Delta x}, \quad (2)$$

where R is the gas constant for dry air, and T_v is the absolute virtual temperature. For p = 700 mb, T_v = 273 K, the constants are

$$\frac{RT_v}{p^2} \sim 1.6 \times 10^{-3}\ \mathrm{kg^{-1}\ m^3\ mb^{-1}},$$

$$\frac{R}{P} \sim 4.1 \times 10^{-3}\ \mathrm{kg^{-1}\ m^3\ k^{-1}}.$$

Estimates of the terms in (1), using (2) are shown in Table 1. It is obvious that the direct influence of Coriolis terms is negligible on the time scale over which we are concerned. As concluded by Ray *et al.* (1976), the tilting term emerges as the likely candidate for the major source of vorticity amplification in mid-levels, with the stretching term a close rival, especially in low levels. However, for the given range of values, the solenoid term is a potential modulating influence and should not be casually dismissed, as is often done. This has been noted by Morton (1966, pp. 169–170), who disregarded solenoidal effects only because the observations available to him did not show the presence of the persistent baroclinic zone separating updraft from downdraft. In fact, the measurements of Heymsfield *et al.* (1978) have shown that horizontal temperature differences can exceed 5°C over a distance of <0.5 km for cumulus congestus. In a severe storm, the development of a cold rear flank downdraft, in close proximity to an intense updraft, probably enhances this gradient.

7. Conclusions and implications

After reviewing many studies of supercell storms observed primarily over the Great Plains of the United States, a consistent pattern of tornadogene-

sis is obtained. First, the mesocyclone structure changes from an initial intense rotating updraft (producing very large hail and funnel clouds) to a divided mesocyclone, with downdraft on the rear flank and updraft on the forward flank. Second, tornadoes—at least the more significant tornadoes—develop only after the mesocyclone forms the divided structure, i.e., is centered on the interface separating positive and negative vertical velocity. Third, while the rear flank downdraft plays a major role in tornadogenesis, it also contributes to initial disruption of the updraft and, ultimately, to storm collapse and tornado dissipation by cutting off the inflow. In its final phases, the circulation is dominated by downdrafts and precipitation. If severe weather production is to resume, new updraft must develop on the flanks, often in association with the accelerating outflow boundary.

The first and second observations suggest a revision may be needed in the theory of tornadic vorticity generation. The leading candidate in a revised theory is likely to be tilting of horizontal vorticity into the vertical but this may be modulated by stretching of the vortex tubes and, possibly, by the horizontal solenoid field associated with the development of a cold, relatively dense rear flank downdraft. This downdraft forms on the upwind side of the updraft, creating a vertically continuous (although perhaps somewhat tilted) zone of strong density and vertical velocity gradient as it descends to the surface. The initial mesocyclone which is centered on the intense updraft, however, may result from convergence of ambient vorticity. Nevertheless, this convergence may not be the source of tornadic vorticity.

Potential short-range forecasting applications of this concept exist if the model is verified. It has been suggested that the development of the most significant tornadoes is associated with strong relative winds at 7 to 10 km AGL and ingestion of dry, mid-level air into the storm's rear flank. Thus, once a strong thunderstorm exists, its motion relative to the upper mid-level environmental flow can be used as a criterion for separating potentially tornadic from non-tornadic storms. In a somewhat longer range forecast problem, should this concept be verified, flow strength at 7 to 10 km AGL can be added to forecast criteria for tornadoes. The model can also explain the known requirement for the presence of dry mid-level air upstream from a severe storm threat area. Conversely, the absence of strong flow at upper mid-levels implies a reduced threat of tornadoes, even when severe thunderstorms are possible. Finally, since strong surface wind gusts in both tornadic and nontornadic storms are directly related to downdraft strength, the potential for damaging winds (downbursts) should also be related to the development of a rear flank downdraft. These applications are being pursued.

TABLE 1. Estimates of terms in vorticity equation for given ranges of values.

Coriolis Terms

$v(\partial f/\partial y)$

	v (m s^{-1})		
	10	20	50
	2.0×10^{-10}	4.0×10^{-10}	1.0×10^{-9}

fD

D (s^{-1})			
1.0×10^{-3}	2.0×10^{-3}	5.0×10^{-3}	1.0×10^{-2}
1.0×10^{-7}	2.0×10^{-7}	5.0×10^{-7}	1.0×10^{-7}

Stretching Term

$\Delta v/D$

	Δv (m s^{-1})		
D (s^{-1})	10	20	50
1.0×10^{-3}	1.0×10^{-2}	2.0×10^{-2}	5.0×10^{-2}
2.0×10^{-3}	2.0×10^{-2}	4.0×10^{-1}	1.0×10^{-1}
5.0×10^{-3}	5.0×10^{-2}	1.0×10^{-1}	2.5×10^{-1}
1.0×10^{-2}	1.0×10^{-1}	2.0×10^{-1}	5.0×10^{-1}

Tilting Term

$\Delta w \partial v/\partial z$

	Δw (m s^{-1})		
$\partial v/\partial z$ (s^{-1})	10	20	50
5.0×10^{-3}	5.0×10^{-2}	1.0×10^{-1}	2.5×10^{-1}
1.0×10^{-2}	1.0×10^{-1}	2.0×10^{-1}	5.0×10^{-1}
2.0×10^{-2}	2.0×10^{-1}	4.0×10^{-1}	1.0×10^{0}

Solenoid Terms at $p = 700$ mb

$\left(\frac{R}{P}\right)\Delta T_v(\partial p/\partial y)$

	ΔT_v (K), $\Delta p = 0$			
$\partial p/\partial y$ (mb km^{-1})	1	2	5	10
0.5	2.1×10^{-4}	4.1×10^{-4}	1.0×10^{-3}	2.1×10^{-3}
1.0	4.1×10^{-4}	8.2×10^{-4}	2.1×10^{-3}	4.1×10^{-3}
2.0	8.2×10^{-4}	1.6×10^{-3}	4.1×10^{-3}	8.2×10^{-3}
5.0	2.1×10^{-3}	4.1×10^{-3}	1.0×10^{-2}	2.1×10^{-2}

$\left(\frac{RT_v}{p^2}\right)\Delta p(\partial p/\partial y)$

	Δp (mb), $T_v = 273$ K, $\Delta T_v = 0$			
$\partial p/\partial y$ (mb km^{-1})	1	2	5	10
0.5	8.0×10^{-5}	1.6×10^{-4}	4.0×10^{-4}	8.0×10^{-4}
1.0	1.6×10^{-4}	3.2×10^{-4}	8.0×10^{-4}	1.6×10^{-4}
2.0	3.2×10^{-4}	6.4×10^{-4}	1.6×10^{-4}	3.2×10^{-4}
5.0	8.0×10^{-3}	1.6×10^{-3}	4.0×10^{-3}	8.0×10^{-3}

The supercell model we have presented here represents an attempt to incorporate the available observations of evolving supercell tornadic storms into a coherent structure. Although no new data have been presented, it is felt that sufficient evidence already exists for the presence of the rear flank downdraft and divided mesocyclone to try to incorporate them into the supercell model. The principal gaps in our knowledge lie in the thermodynamic structure above the surface and in the kinematic features outside of the storm's precipitation-filled volume. Although aircraft penetrations have been made that are not inconsistent with the model presented, they lack sufficient vertical and temporal sampling resolution to provide the needed detail. Also, there is a real need for sampling the upstream near-storm environment in much greater detail, to resolve the origins and characteristics of the rear flank downdraft.

It is noteworthy that these gaps can possibly be filled by the intensive effort of the Severe Environmental Storms and Mesoscale Experiment (Lilly, 1976). The Doppler radar, rawinsonde, surface, visual, and aircraft observations may well be adequate to confirm or refute the validity of our model. Should the basic features of the model be confirmed by the new data, we propose that sources for tornadic vorticity be reevaluated.

Acknowledgments. The authors are indebted to the many researchers who have spent unnumbered hours developing the careful analyses of the data and observations we have referenced. We further recognize: Dr. Joseph T. Schaefer of the Techniques Development Unit, Dr. Robert Davies-Jones and Mr. Don Burgess of the National Severe Storms Laboratory for their helpful discussions and review of the manuscript, the anonymous reviewers for their beneficial comments on the manuscript and concepts and, finally, Margaret Coonfield and Beverly Lambert for their excellence and patience in manuscript typing.

REFERENCES

Alberty, R. L., 1969: A proposed mechanism for cumulonimbus persistence in the presence of strong vertical shear. *Mon. Wea. Rev.*, **97**, 590–596.

Barcilon, A. I., and P. G. Drazin, 1971: Dust devil formation. *Geophys. Fluid. Dyn.*, **4**, 147–158.

Barnes, S. L., 1978: Oklahoma thunderstorms on 29–30 April 1970. Part 1: Morphology of a tornadic storm. *Mon. Wea. Rev.*, **106**, 673–684.

Beebe, R. G., 1959: Notes on Scottsbluff, Nebraska tornado, 27 June 1955. *Bull. Amer. Meteor. Soc.*, **40**, 109–116.

Bonesteele, R. G., and Y. J. Lin, 1978: A study of updraft-downdraft interaction based on perturbation pressure and single-Doppler radar data. *Mon. Wea. Rev.*, **106**, 62–68.

Brandes, E. A., 1977a: Flow in severe thunderstorms observed by dual-Doppler radar. *Mon. Wea. Rev.*, **105**, 113–120.

——, 1977b: Gust front evolution and tornadogenesis as viewed by Doppler radar. *J. Appl. Meteor.*, **16**, 333–338.

——, 1978: Mesocyclone evolution and tornadogenesis: Some observations. *Mon. Wea. Rev.*, **106**, 995–1011.

Brooks, E. M., 1949: The tornado cyclone. *Weatherwise*, **2**, 32–33.

Brown, R. A., D. W. Burgess and K. C. Crawford, 1973: Twin tornado cyclones within a severe thunderstorm: Single-Doppler radar observations. *Weatherwise*, **26**, 63–71.

——, L. R. Lemon and D. W. Burgess, 1978: Tornado detection by pulsed Doppler radar. *Mon. Wea. Rev.*, **106**, 29–38.

Browning, K. A., 1964: Airflow and precipitation trajectories within severe local storms which travel to the right of the winds. *J. Atmos. Sci.*, **21**, 634–639.

——, 1977: The structure and mechanism of hailstorms. *Hail: A Review of Hail Science and Hail Suppression*, G. B. Foote and C. A. Knight, Eds., *Meteor. Monogr.*, No. 38, 1–39.

——, and G. B. Foote, 1976: Airflow and hail growth in supercell storms and some implications for hail suppression. *Quart. J. Roy. Meteor. Soc.*, **102**, 499–534.

Burgess, D. W., and R. A. Brown, 1973: The structure of a severe right moving thunderstorm: New single-Doppler radar evidence. *Preprints Eighth Conf. on Severe Local Storms*, Denver, Amer. Meteor. Soc., 99–106.

——, L. D. Hennington, R. J. Doviak and P. S. Ray, 1976: Multimoment Doppler display for severe storm identification. *J. Appl. Meteor.*, **15**, 1302–1306.

——, R. A. Brown, L. R. Lemon and C. R. Safford, 1977: Evolution of a tornadic thunderstorm. *Preprints Tenth Conf. on Severe Local Storms*, Omaha, Amer. Meteor. Soc., 84–89.

Byers, H. R., and R. R. Braham, 1949: *The Thunderstorm*. U.S. Govt. Printing Office, Washington, DC, 287 pp.

Charba, J., and Y. Sasaki, 1971: Structure and movement of the severe thunderstorms of 3 April 1964 as revealed from radar and surface mesonetwork data analysis. *J. Meteor. Soc. Japan*, **49**, 191–214.

Chisholm, A. J., 1973: Radar case studies and airflow models. *Alberta Hailstorms, Meteor. Monogr.*, No. 36, Amer. Meteor. Soc., 1–36.

Clark, T. L., and R. List, 1971: Dynamics of a falling particle zone. *J. Atmos. Sci.*, **28**, 718–727.

Danielson, E. F., 1975: A conceptual theory of tornadogenesis based on macro, meso- and microscale processes. *Preprints Ninth Conf. on Severe Local Storms*, Norman, Amer. Meteor. Soc., 376–383.

Darkow, G. L., and J. C. Roos, 1970: Multiple tornado producing thunderstorms and their apparent cyclic variations in intensity. *Preprints Fourteenth Conf. on Radar Meteorology*, Tucson, Amer. Meteor. Soc., 305–308.

——, and D. W. McCann, 1979: Relative environmental winds for 121 tornado-bearing storms. Submitted for publication to *Mon. Wea. Rev.*

Davies-Jones, R. P., and E. Kessler, 1974: Tornadoes. *Weather and Climate Modification*, W. N. Hess, Ed., John Wiley and Sons, 842 pp. (see Chap. 16, 552–595).

Donaldson, R. J., Jr., 1978: Observations of the Union City tornadic storm by plan shear indicator. *Mon. Wea. Rev.*, **106**, 39–47.

Flora, S. D., 1954: *Tornadoes of the United States*. University of Oklahoma Press, 221 pp.

Fujita, T., 1960: A detailed analysis of the Fargo tornadoes of June 20, 1957. U.S. Weather Bureau Res. Pap. No. 42, 67 pp.

——, 1973: Proposed mechanism of tornado formation from rotating thunderstorm. *Preprints Eighth Conf. on Severe Local Storms*, Denver, Amer. Meteor. Soc., 191–196.

Garrett, R. A., and V. D. Rockney, 1962: Tornadoes in northeastern Kansas, May 19, 1960. *Mon. Wea. Rev.*, **90**, 231–240.

Golden, J. T., and D. Purcell, 1977: Photogrammetric velocities for the Great Bend, Kansas tornado of 30 August, 1974: Accelerations and asymmetrics, *Mon. Wea. Rev.*, **105**, 485–492.

——, and ——, 1978: Airflow characteristics around the Union City tornado. *Mon. Wea. Rev.*, **106**, 22–38.

Gubin, V. I., 1962: *Hydrodynamic Theory of Frontogenesis.* Translated by Israel Program for Scientific Translations, Jerusalem, 96 pp.

Haglund, G. T., 1969: A study of severe local storm of 16 April 1967. ESSA Tech. Memo. ERLTM-NSSL 44, 54 pp. [NTIS No. PB188315].

Heymsfield, A. J., P. N. Johnson and J. E. Dye, 1978: Observations of moist adiabatic ascent in northeast Colorado cumulus congestus clouds. *J. Atmos. Sci.*, **35,** 1689–1703.

Huff, F. A., H. W. Hiser and S. G. Bigler, 1954: Study of an Illinois tornado using radar, synoptic weather and field survey data. Rep. of Investigation No. 22, Illinois State Water Survey, 73 pp.

Kamburova, P. L., and F. H. Ludlam, 1966: Rainfall evaporation in thunderstorm downdrafts. *Quart. J. Roy. Meteor. Soc.*, **92,** 510–518.

Kessler, E., 1970: Thunderstorms over Oklahoma 22 June 1969. *Weatherwise*, **23,** 56–69.

Klemp, J. B., and R. B. Wilhelmson, 1978: Simulations of right- and left-moving storms produced through storm splitting. *J. Atmos. Sci.*, **35,** 1097–1110.

Lemon, L. R., 1970: Formation and emergence of an anticyclonic eddy within a severe thunderstorm as revealed by radar and surface data. *Preprints Fourteenth Conf. on Radar Meteorology*, Tucson, Amer. Meteor. Soc., 323–328.

——, 1974: Interaction of two convective scales within a severe thunderstorm: A case study. NOAA Tech. Memo. ERL-NSSL, 71, 43 pp. [NTIS No. COM-74-11642/AS].

——, 1976: The flanking line, a severe thunderstorm intensification source. *J. Atmos. Sci.*, **33,** 686–694.

——, 1977: New severe thunderstorm radar identification techniques and warning criteria: A preliminary report. NOAA Tech. Memo. NWS-NSSFC 1, 60 pp. [NTIS No. PB-273049.]

——, D. W. Burgess and R. A. Brown, 1975: Tornado production and storm sustenance. *Preprints Ninth Conf. on Severe Local Storms*, Norman, Amer. Meteor. Soc., 100–104.

——, —— and ——, 1978: Tornadic storm airflow and morphology derived from single Doppler radar measurements. *Mon. Wea. Rev.*, **106,** 48–61.

——, R. J. Donaldson, Jr., D. W. Burgess and R. A. Brown, 1977: Doppler radar application to severe thunderstorm study and potential real-time warning. *Bull. Amer. Meteor. Soc.*, **58,** 1187–1193.

Lilly, D. K., 1976: Project Severe Environmental Storms and Mesoscale Experiment (SESAME). Project Development Plan, Environmental Research Laboratories, NOAA, Boulder, 60 pp.

Ludlam, F. H., 1963: *Severe Local Storms. A Review. Meteor. Monogr.*, No. 27, Amer. Meteor. Soc., 1–30.

Marwitz, J. D., 1972a: The structure and motion of severe hailstorms. Part I: Supercell storms. *J. Appl. Meteor.*, **11,** 166–179.

——, 1972b: The structure and motion of severe hailstorms. Part III: Severely sheared storms. *J. Appl. Meteor.*, **11,** 189–201.

——, A. H. Auer, Jr. and D. L. Veal, 1972: Locating the organized updraft on severe thunderstorms. *J. Appl. Meteor.*, **11,** 236–238.

Melbourne, W. H., and P. N. Joubert, 1971: Problems of wind flow at the base of tall buildings. *Preprints 3rd Int. Conf. on Wind Effects on Building and Structures*, Sci. Council of Japan, University of Tokyo, 105–114.

Milne-Thomson, L. M., 1968: *Theoretical Hydrodynamics*, 5th ed. Macmillan, 355 pp.

Moller, A., C. Doswell, J. McGinley, S. Tegtmeier and R. Zipser, 1974: Field observations of the Union City tornado in Oklahoma. *Weatherwise*, **27,** 68–77.

Morton, B. R., 1966: Geophysical vortices. *Progress in Aeronautical Sciences*, Vol. 7, Pergamon Press, 145–192.

Nelson, S. P., 1976: Characteristics of multicell and supercell hailstorms in Oklahoma. *Proc. Second WMO Conf. on Weather Modification*, WMO-443, Boulder, 335–340.

——, 1977: Rear flank downdraft: A hailstorm intensification mechanism. *Preprints 10th Conf. on Severe Local Storms*, Omaha, Amer. Meteor. Soc., 521–525.

Newton, C. W., 1963: Dynamics of severe convective storms. *Meteor. Monogr.*, No. 27, Boston, Amer. Meteor. Soc., 33–58.

——, and H. R. Newton, 1959: Dynamical interactions between large convective clouds and environment with vertical shear. *J. Meteor.*, **16,** 483–496.

Palmén, E., and C. W. Newton, 1969: *Atmospheric Circulation Systems.* Academic Press, 603 pp.

Peterson, R. E., 1976: The Sunray tornado. *Bull. Amer. Meteor. Soc.*, **57,** 805–807.

Petterssen, S., and J. M. Austin, 1942: Fronts and frontogenesis in relation to vorticity. *Pap. Phys. Ocean. Meteor.*, **7,** Cambridge and Woods Hole, 37 pp.

Ramond, D., 1978: Pressure perturbations in deep convection: An experimental study. *J. Atmos. Sci.*, **35,** 1704–1711.

Ray, P. S., and K. K. Wagner, 1976: Multiple Doppler radar observations of storms. *Geophys. Res. Lett.*, **3,** 189–191.

——, C. E. Hane, R. P. Davies-Jones and R. L. Alberty, 1976: Tornado-parent storm relationship deduced from a dual-Doppler radar analysis. *Geophys. Res. Lett.*, **3,** 721–723.

Sawyer, J. S., 1949: Cooling of air by rain as a factor in convection. *Prof. Note*, No. 96, Met. Office, London, 11 pp.

Schlesinger, R. E., 1978: A three-dimensional numerical model of an isolated thunderstorm: Part I, Comparative experiments for variable ambient wind shear. *J. Atmos. Sci.*, **35,** 690–713.

Stanford, J. L., 1977: *Tornado: Accounts of Tornadoes in Iowa.* Iowa State University Press, 120 pp.

Williams, D. T., 1963: The thunderstorm wake of May 4, 1961. National Severe Storms Project Rep. No. 18, 23 pp. [NTIS No. PB 168223.]

Wise, A. F. E., 1971: Effects due to groups of buildings. *Phil. Trans. Roy. Soc. London,* **A269,** 469–485.

Van Tassel, E. L., 1955: The North Platte Valley tornado outbreak of June 27, 1955. *Mon. Wea. Rev.*, **83,** 255–264.

Zipser, E. J., 1977: Mesoscale and convective-scale downdrafts as distinct components of squall-line structure. *Mon. Wea. Rev.*, **105,** 1568–1589.